Journal of Computational Physics **172,** 166–187 (2001)
doi:10.1006/jcph.2001.6818, available online at http://www.idealibrary.com on IDEAL®

Conservative Numerical Schemes for the Vlasov Equation

Francis Filbet,* Eric Sonnendrücker,† and Pierre Bertrand‡

*IECN–INRIA Project Numath, Université de Nancy I, BP 239, 54506 Vandœuvre-lès-Nancy Cedex, France; †IRMA, Université Louis Pasteur, 7 Rue R Descartes, 67084 Strasbourg, France; and ‡LPMI, Université de Nancy I, BP 239, 54506 Vandœuvre-lès-Nancy Cedex, France
E-mail: sonnen@math.u-strasbg.fr

Received January 4, 2001; revised April 18, 2001

A new scheme for solving the Vlasov equation using a phase space grid is proposed. The algorithm is based on the conservation of the flux of particles, and the distribution function is reconstructed using various techniques that allow control of spurious oscillations or preservation of the positivity. Several numerical results are presented in two- and four-dimensional phase space and the scheme is compared with the semiLagrangian method. This method is almost as accurate as the semi-Lagrangian one, and the local reconstruction technique is well suited for parallel computation. © 2001 Academic Press

The Vlasov equation describes the evolution of a system of particles under the effects of self-consistent electromagnetic fields. The unknown $f(t, x, v)$, depending on the time t, the position x, and the velocity v, represents the distribution function of particles (electrons, ions, . . .) in phase space. This model can be used for the study of beam propagation or collisionless plasma.

The numerical resolution of the Vlasov equation is usually performed by particle methods (PIC) which consist of approximating the plasma by a finite number of macro-particles. The trajectories of these particles are computed from the characteristic curves given by the Vlasov equation, whereas self-consistent fields are computed on a mesh of the physical space. This method allows us to obtain satisfying results with a small number of particles (see Birdsall and Langdon for more details [1]). However, it is well known that the numerical noise inherent to the particle method becomes too significant to allow a precise description of the distribution function in phase space. Moreover, the numerical noise only decreases in $1/\sqrt{N}$ when the number of particles N is increased. To remedy this problem, methods discretizing the Vlasov equation on a mesh of phase space have been proposed. Among them, the Fourier–Fourier transform is based on a fast Fourier transform of the distribution function in phase space, but this method is only valid for periodic boundary conditions

0021-9991/01 $35.00

[8, 9]. Consequently, for nonperiodic boundary conditions, Gibbs oscillations form at the boundary of the grid and become a source of spurious oscillations which propagate into the distribution function. A finite element method has also been proposed [16, 17]. This method is well suited to handling complicated boundaries which may arise in many practical applications, but it requires the numerical resolution of a system which is inconvenient to use to deal with the Vlasov equation in high dimension. The semiLagrangian method, which consists of computing the distribution function at each grid point by following the characteristic curves backward, is also used. To compute the origin of the characteristic, a high-order interpolation method is needed. E. Sonnendrücker *et al*. proposed the cubic spline reconstruction which gives very good results [13, 14], but the use of spline interpolation destroys the local character of the reconstruction. Nakamura and Yabe also presented the cubic interpolated propagation (CIP) method based on the approximation of the gradients of the distribution function in order to use a Hermite interpolation [15]. This method is very expensive in memory computation since it needs the storage of f, $\nabla_x f$, and $\nabla_v f$. Another scheme for the Vlasov equation is the flux corrected transport (FCT) [3, 4] or more recently the flux balance method (FBM) [6]: the basic idea of this method is to compute the average of the Vlasov equation solution in each cell of the phase space grid by a conservative method.

One of the common flaws of these algorithms is the nonpreservation of the positivity which is inconvenient for lengthy simulations since numerical oscillations develop. The goal of this paper is to propose a new scheme, the positive and flux conservative (PFC) method, which gives a good approximation of the distribution function, the conservation of mass, and the preservation of positivity. Moreover, the use of local interpolation allows straightforward and scalable parallel computation.

This paper is organized as follows. In the first part, we briefly describe the Vlasov equation, recalling some properties of the solution, like the conservation of the entropy, L^p norms, and the energy. Then, we present the conservative method for the discretization of a transport equation, using the characteristic curves, and we give various reconstruction techniques which enable us to control spurious oscillations. In the last section, we present numerical results in the two- and four-dimensional phase space to compare the different schemes with the semiLagrangian method.

1. THE VLASOV EQUATION

The evolution of the density of particles $f(t, x, v)dx\,dv$ in the phase space $(x, v) \in \mathbb{R}^d \times \mathbb{R}^d$, $d = 1, \ldots 3$, is given by the Vlasov equation

$$\frac{\partial f}{\partial t} + v \cdot \nabla_x f + F(t, x, v) \cdot \nabla_v f = 0, \tag{1}$$

where the force field $F(t, x, v)$ is coupled with the distribution function f giving a nonlinear system. We mention the well known Vlasov–Poisson (VP) and Vlasov–Maxwell (VM) models describing the evolution of particles under the effects of self-consistent electromagnetic fields: we first define the charge density $\rho(t, x)$ and current density $j(t, x)$ by

$$\rho(t, x) = q \int_{\mathbb{R}^d} f(t, x, v)\, dv, \quad j(t, x) = q \int_{\mathbb{R}^d} v f(t, x, v)\, dv, \tag{2}$$

where q is the single charge. The force field is given for the Vlasov–Poisson model by

$$F(t,x,v) = \frac{q}{m}E(t,x), \quad E(t,x) = -\nabla_x \phi(t,x), \quad -\Delta_x \phi = \frac{\rho}{\varepsilon_0}, \tag{3}$$

where m represents the mass of one particle. For the Vlasov–Maxwell system, we have

$$F(t,x,v) = \frac{q}{m}(E(t,x) + v \wedge B(t,x)), \tag{4}$$

and E, B are solutions of the Maxwell equations

$$\begin{cases} \frac{\partial E}{\partial t} - c^2 \operatorname{curl} B = -\frac{j}{\varepsilon_0}, \\ \frac{\partial B}{\partial t} + \operatorname{curl} E = 0, \\ \operatorname{div} E = \frac{\rho}{\varepsilon_0}, \quad \operatorname{div} B = 0, \end{cases} \tag{5}$$

with the compatibility condition

$$\frac{\partial \rho}{\partial t} + \operatorname{div} j = 0, \tag{6}$$

which is verified by the Vlasov equation solution.

We now recall some classical a priori estimates on the VP and VM systems. First of all, assuming the initial data $f_0(x,v)$ is positive, the solution $f(t,x,v)$ remains positive for all t. Next, observing that $\operatorname{div}_{x,v}(v, F(t,x,v)) = 0$, we immediately deduce that for all functions $\beta \in C^1(\mathbb{R}^+, \mathbb{R}^+)$,

$$\frac{d}{dt}\int_{\mathbb{R}^d \times \mathbb{R}^d} \beta(f(t,x,v))\,dx\,dv = 0, \quad \forall t \in \mathbb{R}^+.$$

In particular all L^p norms, for $1 \le p \le +\infty$, are preserved. Moreover, taking $\beta(r) = r\ln(r)$, we obtain the conservation of the kinetic entropy

$$\frac{d}{dt}H(t) = \frac{d}{dt}\int_{\mathbb{R}^d \times \mathbb{R}^d} f(t,x,v)\ln(f(t,x,v))\,dx\,dv = 0, \quad \forall t \in \mathbb{R}^+.$$

Next, multiplying the Vlasov equation by $|v|^2$ and integrating by parts, we find the conservation of energy for the VP system,

$$\frac{d}{dt}\int_{\mathbb{R}^d \times \mathbb{R}^d} f(t,x,v)|v|^2\,dx\,dv + \int_{\mathbb{R}^d} |E(t,x)|^2\,dx = 0, \quad \forall t \in \mathbb{R}^+,$$

and for the VM system,

$$\frac{d}{dt}\int_{\mathbb{R}^d \times \mathbb{R}^d} f(t,x,v)|v|^2\,dx\,dv + \int_{\mathbb{R}^d} |E(t,x)|^2 + |B(t,x)|^2\,dx = 0, \quad \forall t \in \mathbb{R}^+.$$

Finally, note that the Vlasov equation also preserves mass and impulsion:

$$\frac{d}{dt}\int_{\mathbb{R}^d \times \mathbb{R}^d} f(t,x,v)\begin{pmatrix}1\\ v\end{pmatrix}dx\,dv = 0, \quad \forall t \in \mathbb{R}^+.$$

2. THE CONSERVATIVE METHOD

In this section, we introduce conservative discretizations of the Vlasov equation and propose several reconstruction techniques. Unlike classical Eulerian algorithms such as finite difference or finite volume schemes, this method is not restricted by a CFL (Courant–Friedrichs–Levy) condition on the time step. The Vlasov equation coupled with the Poisson equation or the Maxwell system often contains filamentation, which is one of the major issues one has to deal with when constructing a numerical scheme. Indeed, the distribution function $f(t, x, v)$ is constant along the characteristic curves, which become close, so that phase space regions where $f(t, x, v)$ has different values come close together and steep gradients are generated. At some time in the simulation, the phase space grid becomes too coarse to follow these thin filaments. The various gridded methods briefly presented in the introduction have no mechanism to distinguish numerical oscillations and filamentation. The algorithm should effectively be high order in regions of the problem where the concept of order is related usefully to accuracy, and should control oscillations where gradients are large or where the distribution function goes to zero. The conservative method presented below is derived from these requirements.

The starting point of our method is the Flux Balance method [6], discretizing the Vlasov equation in the conservative form: we first observe that by a standard time-splitting scheme, we can restrict ourselves, without loss of generality, to a one-dimensional problem which leads to solving the following problem:

$$\partial_t f + \partial_x(\mathrm{u}(t, x) f) = 0, \quad \forall (t, x) \in \mathbb{R}^+ \times [x_{min}, x_{max}]. \tag{7}$$

We will assume that $\mathrm{u}(t, x)$ is smooth enough; for example u is Lipschitz continuous. Then we can define the characteristic curves solution of the differential system corresponding to the transport equation:

$$\begin{cases} \frac{dX}{ds}(s) = \mathrm{u}(s, X(s)), \\ X(t) = x. \end{cases} \tag{8}$$

Let us denote by $X(s, t, x)$ the solution of (8) and define the Jacobian $J(s, t, x) = \partial_x X(s, t, x)$. In [2], it is proved that $J(s, t, x)$ is positive for all $(s, t, x) \in \mathbb{R}^+ \times \mathbb{R}^+ \times \mathbb{R}$, and the solution of the transport equation (7) can be expressed as

$$f(t, x) = f(s, X(s, t, x)) J(s, t, x), \tag{9}$$

which describes the conservation of particles along the characteristic curves

$$\forall K \subset \mathbb{R}, \qquad \int_K f(t, x)\, dx = \int_{X(s,t,K)} f(s, x)\, dx, \tag{10}$$

where

$$X(s, t, K) = \{y \in \mathbb{R}: \quad y = X(s, t, z); \quad z \in K\}.$$

This property remains true if $d \geq 1$. Now let us introduce a finite set of mesh points $(x_{i+1/2})_{i \in I}$ of the computational domain (x_{min}, x_{max}), which we will denote by $\Delta x = x_{i+1/2} - x_{i-1/2}$, and $C_i = [x_{i-1/2}, x_{i+1/2}]$. Assuming the values of the distribution function

are known at time $t^n = n\Delta t$, we find the new values at time t^{n+1} by integration of the distribution function on each subinterval. Thus, using the conservation of particles (10) and recalling that the Jacobian function $x \mapsto J(t^n, t^{n+1}, x)$ is positive, we have

$$\int_{x_{i-1/2}}^{x_{i+1/2}} f(t^{n+1}, x)\, dx = \int_{X(t^n, t^{n+1}, x_{i+1/2})}^{X(t^n, t^{n+1}, x_{i+1/2})} f(t^n, x)\, dx.$$

Then, we set

$$\Phi_{i+1/2}(t^n) = \int_{X(t^n, t^{n+1}, x_{i+1/2})}^{x_{i+1/2}} f(t^n, x)\, dx$$

to finally obtain the conservative scheme

$$\int_{x_{i-1/2}}^{x_{i+1/2}} f(t^{n+1}, x)\, dx = \Phi_{i-1/2}(t^n) + \int_{x_{i-1/2}}^{x_{i+1/2}} f(t^n, x)\, dx - \Phi_{i+1/2}(t^n). \tag{11}$$

The evaluation of the average of the solution over $[x_{i-1/2}, x_{i+1/2}]$ allows us to ignore small details of the exact solution which may be very costly to compute.

In general, we cannot explicitly compute the characteristic curves; we need to introduce a time discretization of (8). Using a second-order leap-frog scheme, we obtain a fixed point problem, where we look for $x^n = X(t^n, t^{n+1}, x_{i+1/2})$ such that

$$\begin{cases} x_{i+1/2} - x^n = \Delta t u\left(t^{n+1/2}, x^{n+1/2}\right), \\ t^{n+1/2} = t^n + \frac{\Delta t}{2}, \quad x^{n+1/2} = \frac{x_{i+1/2} + x^n}{2}, \end{cases}$$

which can be iteratively solved. Note that most of the time in kinetic transport equations, the time-splitting scheme allows us to avoid this situation since the characteristic curves become straight lines.

The main step is now to choose an efficient method to reconstruct the distribution function from the values in each cell C_i. In [6], E. Fijalkow only used a linear interpolation, but this method does not give a positive scheme and does not control spurious oscillations. The method proposed by Boris and Book [3] or the use of classical slope limiters is too dissipative to give an accurate description of the distribution function. Here, we shall use a reconstruction via a primitive function: let $F(t^n, .)$ be a primitive of the distribution function $f(t^n, .)$, which we denote by

$$f_i^n = \frac{1}{\Delta x} \int_{x_{i-1/2}}^{x_{i+1/2}} f(t^n, x)\, dx.$$

Then we have $F(t^n, x_{i+1/2}) - F(t^n, x_{i-1/2}) = \Delta x f_i^n$, and

$$F\left(t^n, x_{i+1/2}\right) = \Delta x \sum_{k=0}^{i} f_k^n = w_i^n.$$

In the sequel, the time variable t^n only acts as a parameter and will be dropped. We present two different methods of reconstruction.

2.1. The ENO Reconstruction

The ENO (essentially nonoscillatory) method has been introduced by Harten and Osher in [7]. It is often used for the discretization of hyperbolic equations and allows the control of spurious oscillations. Unlike classical conservation laws, the Vlasov equation solution does not develop any shock, but stiff gradients appear in the phase space. Thus, the ENO reconstruction seems to be useful for treating this problem. We first recall the divided difference formula which plays an important role in this method:

$$\begin{aligned} F\left[x_{i+1/2}, x_{i+3/2}, \ldots, x_{i+p+1/2}\right] &= \frac{F\left[x_{i+3/2}, \ldots, x_{i+p+1/2}\right] - F\left[x_{i+1/2}, \ldots, x_{i+p-1/2}\right]}{x_{i+p+1/2} - x_{i+1/2}}, \\ F\left[x_{i+1/2}\right] &= F\left(x_{i+1/2}\right) = w_i. \end{aligned} \tag{12}$$

It also satisfies the properties

- If $F(x) \in C^p([x_{i+1/2}, x_{i+p+1/2}])$, then

$$\exists \zeta \in \left(x_{i+1/2}, x_{i+p+1/2}\right), \quad F\left[x_{i+1/2}, x_{i+3/2}, \ldots, x_{i+p+1/2}\right] = \frac{1}{p!}\frac{d^p F}{dx^p}(\zeta).$$

- If the k-th derivative of $F(x)$ is discontinuous with $0 \le k \le p$ on the interval $[x_{i+1/2}, x_{i+p+1/2}]$, then

$$F\left[x_{i+1/2}, x_{i+3/2}, \ldots, x_{i+p+1/2}\right] = O(\Delta x^{k-p})\left[\omega^{(k)}\right],$$

where $[\omega^{(k)}]$ represents the jump of the k-th derivative. The ENO reconstruction consists of choosing the stencil for which the approximation is the smoothest, i.e., for which the divided difference is the smallest in module: on the interval $[x_{i-1/2}, x_{i+1/2}]$, we first define $q_1(x)$, the polynomial of degree one, interpolating the function $F(x)$ at $x_{i-1/2}$ and $x_{i+1/2}$,

$$q_1(x) = w_{i-1} + \left(x - x_{i-1/2}\right)\frac{w_i - w_{i-1}}{\Delta x};$$

and we set $d_1(i) = i$. Let us assume that we have constructed the polynomial of degree k interpolating the function $F(x)$ at the points

$$x_{d_k(i)-1/2}, \ldots, x_{d_k(i)+k-1/2}.$$

To find the polynomial $q_{k+1}(x)$, we consider $k+2$ points obtained by adding to the previous ones the first point on the left or on the right, and choose the point for which the divided difference is the smallest:

$$d_{k+1}(i) = \begin{cases} d_k(i) - 1 & \text{if } \left|F\left[x_{d_k(i)-3/2}, \ldots, x_{d_k(i)+k-1/2}\right]\right| \le \left|F\left[x_{d_k(i)-1/2}, \ldots, x_{d_k(i)+k+1/2}\right]\right|, \\ d_k(i) & \text{else.} \end{cases}$$

We continue the algorithm until we reach the order we want.

PROPOSITION 2.1. *Let us assume the function $F(x)$ is $r+1$ continuously differentiable and define its piecewise polynomial approximation denoted by $F_h(x)$ such that*

$$\forall x \in \left[x_{i-1/2}, x_{i+1/2}\right], \quad F_h(x) = q_r(x),$$

where $q_r(x)$ is the polynomial of degree r constructed by following the previous method. Then

- $\frac{d^k q_r}{dx^k}(x) = \frac{d^k F}{dx^k}(x) + O(\Delta x^{r+1-k}), \quad 0 \le k \le r,$
- $q_r(x_{j+1/2}) = F(x_{j+1/2}), \quad \forall j \in \{d_{r(i)-1/2}, \ldots, d_{r(i)+r-1/2}\},$
- *$q_r(x)$ is an essentially nonoscillatory reconstruction in the sense that*

$$TV[q_r(.)] \le TV[F(.)] + O(\Delta x^{r+1}),$$

where the total variation (TV) of a function $F(.)$ is the number given by the following limit:

$$TV[F(.)] = \limsup_{\varepsilon \to 0} \frac{1}{\varepsilon} \int |F(x+\varepsilon) - F(x)|\, dx.$$

The last inequality implies that spurious oscillations are controlled at the order $r+1$ (see [7]). From this high-order-accurate reconstruction, we can define the quantity $\Phi_{i+1/2}(t^n)$ by

$$\Phi_{i+1/2}(t^n) = \int_{X(t^n, t^{n+1}, x_{i+1/2})}^{x_{i+1/2}} f(t^n, x)\, dx = F_h\left(x_{i+1/2}\right) - F_h\left(X\left(t^n, t^{n+1}, x_{i+1/2}\right)\right).$$

This method has been implemented up to the fourth order. It is not positive but allows us to control spurious oscillations.

2.2. The Positive and Flux Conservative Method

As before, we use the reconstruction via primitive function, but the stencil is now fixed. To ensure the preservation of positivity and the maximum principle, we introduce a slope corrector. Indeed, it is only by sacrificing the high order requirement when the gradients are very steep that we can hope to obtain a positive algorithm. In the following, we denote $f_\infty = \max_{j \in I}\{f_j\}$.

The Second-Order Approximation

Let us assume for simplicity the propagating velocity $u(t, x)$ is positive. Then we build a first approximation on the interval $[x_{i-1/2}, x_{i+1/2}]$ using the points $\{x_{i-1/2}, x_{i+1/2}, x_{i+3/2}\}$;

$$\tilde{F}_h(x) = w_{i-1} + \left(x - x_{i-1/2}\right) f_i + \frac{1}{2}\left(x - x_{i-1/2}\right)\left(x - x_{i+1/2}\right)\frac{f_{i+1} - f_i}{\Delta x},$$

where $w_i - w_{i-1} = \Delta x f_i$. Thus by differentiation we obtain a second-order-accurate approximation of the distribution function on the interval $[x_{i-1/2}, x_{i+1/2}]$:

$$\tilde{f}_h(x) = \frac{d\tilde{F}_h}{dx}(x) = f_i + (x - x_i)\frac{f_{i+1} - f_i}{\Delta x}.$$

But this approximation does not satisfy the maximum principle, and spurious oscillations may occur. So we introduce a slope corrector,

$$\epsilon_i = \begin{cases} \min(1; 2f_i/(f_{i+1} - f_i)) & \text{if } f_{i+1} - f_i > 0, \\ \min(1; -2(f_\infty - f_i)/(f_{i+1} - f_i)) & \text{if } f_{i+1} - f_i < 0, \end{cases} \tag{13}$$

and finally obtain the following approximation:

$$f_h(x) = f_i + \epsilon_i (x - x_i) \frac{f_{i+1} - f_i}{\Delta x}, \quad \forall x \in \left[x_{i-1/2}, x_{i+1/2}\right]. \tag{14}$$

From this construction, the following proposition is obvious.

PROPOSITION 2.2. *The approximation defined by* (14) *satisfies*

- *The conservation of the average*: *for all* $i \in I$, $\int_{x_{i-1/2}}^{x_{i+1/2}} f_h(x)\,dx = \Delta x f_i$,
- *The maximum principle*: *for all* $x \in (x_{min}, x_{max})$, $0 \le f_h(x) \le f_\infty$.

Moreover, if we assume the total variation of the distribution function $f(x)$ *is bounded, then we obtain the global estimate*:

$$\int_{x_{min}}^{x_{max}} |f_h(x) - \tilde{f}_h(x)|\,dx \le \Delta x \sum_i (1 - \epsilon_i)|f_{i+1} - f_i| \le TV(f)\Delta x.$$

Now we can define an approximation of the flux $\Phi_{i+1/2}(t^n)$. We first find the cell C_j such that $X(t^n, t^{n+1}, x_{i+1/2}) \in C_j$ and set $\alpha_i = x_{j+1/2} - X(t^n, t^{n+1}, x_{i+1/2})$, which satisfies $0 \le \alpha_i \le \Delta x$. Then

$$\Phi_{i+1/2}(t^n) = \int_{x_{j+1/2}-\alpha_i}^{x_{i+1/2}} f(t^n, x)\,dx = \alpha_i \left[f_j + \frac{\epsilon_j}{2}\left(1 - \frac{\alpha_i}{\Delta x}\right)(f_{j+1} - f_j)\right] + \Delta x \sum_{k=j+1}^{i} f_k.$$

By symmetry, we find an approximation of $\Phi_{i+1/2}(t^n)$ when the propagating velocity $u(t, x)$ is negative. We set $\alpha_i = x_{j-1/2} - X(t^n, t^{n+1}, x_{i+1/2})$, and then $-\Delta x \le \alpha_i \le 0$ and

$$\Phi_{i+1/2}(t^n) = \int_{x_{j-1/2}-\alpha_i}^{x_{i+1/2}} f(t^n, x)\,dx = \alpha_i \left[f_j - \frac{\epsilon_j}{2}\left(1 + \frac{\alpha_i}{\Delta x}\right)(f_j - f_{j-1})\right] + \Delta x \sum_{k=i+1}^{j-1} f_k,$$

where ϵ_j is given by

$$\epsilon_j = \begin{cases} \min(1; 2(f_\infty - f_j)/(f_j - f_{j-1})) & \text{if } f_j - f_{j-1} > 0, \\ \min(1; -2f_j/(f_j - f_{j-1})) & \text{if } f_j - f_{j-1} < 0. \end{cases} \tag{15}$$

Third-Order Approximation

We now extend the previous method for the third-order reconstruction. On the interval $[x_{i-1/2}, x_{i+1/2}]$, we use the stencil $\{x_{i-3/2}, x_{i-1/2}, x_{i+1/2}, x_{i+3/2}\}$ to approximate the primitive, and as before, we introduce a slope corrector to finally obtain for all $x \in C_i$,

$$\begin{aligned} f_h(x) = f_i &+ \frac{\epsilon_i^+}{6\Delta x^2}\left[2(x - x_i)(x - x_{i-3/2}) + (x - x_{i-1/2})(x - x_{i+1/2})\right](f_{i+1} - f_i) \\ &+ \frac{\epsilon_i^-}{6\Delta x^2}\left[2(x - x_i)(x - x_{i+3/2}) + (x - x_{i-1/2})(x - x_{i+1/2})\right](f_i - f_{i-1}), \end{aligned} \tag{16}$$

with

$$\epsilon_i^+ = \begin{cases} \min(1; 2f_i/(f_{i+1} - f_i)) & \text{if } f_{i+1} - f_i > 0, \\ \min(1; -2(f_\infty - f_i)/(f_{i+1} - f_i)) & \text{if } f_{i+1} - f_i < 0, \end{cases} \tag{17}$$

and

$$\epsilon_i^- = \begin{cases} \min(1; 2(f_\infty - f_i)/(f_i - f_{i-1})) & \text{if } f_i - f_{i-1} > 0, \\ \min(1; -2f_i/(f_i - f_{i-1})) & \text{if } f_i - f_{i-1} < 0. \end{cases} \tag{18}$$

PROPOSITION 2.3. *The approximation of the distribution function* $f_h(x)$ *defined by* (16)–(18) *constructed using the third-order method satisfies*

- *The conservation of the average*: *for all* $i \in I$, $\int_{x_{i-1/2}}^{x_{i+1/2}} f_h(x)\,dx = \Delta x f_i$,
- *The maximum principle*: *for all* $x \in (x_{min}, x_{max})$, $0 \le f_h(x) \le f_\infty$.

Moreover, if we assume the total variation of the distribution function $f(x)$ *is bounded, then we obtain the global estimate*

$$\int_{x_{min}}^{x_{max}} |f_h(x) - \tilde{f}_h(x)|\,dx \le 4TV(f)\Delta x,$$

where $\tilde{f}_h$ *denotes the third-order approximation of* f *without the slope corrector.*

Proof. Let us consider $x \in C_i = [x_{i-1/2}, x_{i+1/2}]$ and denote

$$\alpha(x) = \frac{1}{\Delta x^2}\left[2(x - x_i)\left(x - x_{i-3/2}\right) + \left(x - x_{i-1/2}\right)\left(x - x_{i+1/2}\right)\right],$$

$$\beta(x) = \frac{1}{\Delta x^2}\left[2(x - x_i)\left(x - x_{i+3/2}\right) + (x - x_{i-1/2})\left(x - x_{i+1/2}\right)\right].$$

It is easy to check that

$$\int_{x_{i-1/2}}^{x_{i+1/2}} \alpha(x)\,dx = \int_{x_{i-1/2}}^{x_{i+1/2}} \beta(x)\,dx = 0,$$

and the conservation of the average immediately follows. To obtain the preservation of positivity, assuming the values $(f_j)_j$ are positive, we observe that in the cell C_i, the function $\alpha(x)$ is increasing whereas $\beta(x)$ decreases and $\alpha(x), \beta(x) \in [-1, 2]$. Then, we split $f_h(x)$ as the sum of $h(x)$ and $g(x)$ with

$$h(x) = \frac{1}{3}\left[f_i + \frac{\alpha(x)}{2}\epsilon_i^+(f_{i+1} - f_i)\right] \quad \text{and} \quad g(x) = \frac{1}{3}\left[2f_i + \frac{\beta(x)}{2}\epsilon_i^-(f_i - f_{i-1})\right].$$

The function $h(x)$ (*respectively* $g(x)$) is only a combination of f_i and f_{i+1} (*respectively* f_{i-1} and f_i). Then from the value of ϵ_i^+ (*respectively* ϵ_i), it is easy to prove that $h(x)$ (*respectively* $g(x)$) is positive. Using a similar decomposition, we also prove that $f_h(x)$ is bounded by f_∞.

Now, we prove the global estimate on the positive reconstruction:

$$\begin{aligned}\int_{x_{min}}^{x_{max}} |f_h(x) - \bar{f}_h(x)|\,dx &= \sum_i \int_{x_{i-1/2}}^{x_{i+1/2}} |\alpha(x)(1-\epsilon_i^+)[f_{i+1} - f_i] \\ &\quad + \beta(x)(1-\epsilon_i^-)[f_i - f_{i-1}]|\,dx \\ &\le 2\Delta x \sum_i (1-\epsilon_i^+)|f_{i+1} - f_i| + 2\Delta x \sum_i (1-\epsilon_i^-)|f_i - f_{i-1}| \\ &\le 4\Delta x \sum_i |f_{i+1} - f_i| \le 4\Delta x\ TV(f).\end{aligned}$$

■

From this reconstruction, we approximate the quantity $\Phi_{i+1/2}(t^n)$ by looking for the cell C_j such that $X(t^n, t^{n+1}, x_{i+1/2}) \in C_j$ and setting $\alpha_i = x_{j+1/2} - X(t^n, t^{n+1}, x_{i+1/2})$. Then for a positive propagating velocity, we obtain

$$\begin{aligned}\Phi_{i+1/2}(t^n) = \int_{x_{j+1/2}-\alpha_i}^{x_{i+1/2}} f(t^n, x)\,dx = \Delta x \sum_{k=j+1}^{i} f_k + \alpha_i \Bigg[f_j + \frac{\epsilon_j^+}{6}\left(1 - \frac{\alpha_i}{\Delta x}\right)\left(2 - \frac{\alpha_i}{\Delta x}\right) \\ \times (f_{j+1} - f_j) + \frac{\epsilon_j^-}{6}\left(1 - \frac{\alpha_i}{\Delta x}\right)\left(1 + \frac{\alpha_i}{\Delta x}\right)(f_j - f_{j-1}) \Bigg],\end{aligned}$$

and when u(t, x) is negative, we set $\alpha_i = x_{j-1/2} - X(t^n, t^{n+1}, x_{i+1/2})$; then $-\Delta x \le \alpha_i \le 0$ and

$$\begin{aligned}\Phi_{i+1/2}(t^n) = \int_{x_{j-1/2}-\alpha_i}^{x_{i+1/2}} f(t^n, x)\,dx = \Delta x \sum_{k=i+1}^{j-1} f_k + \alpha_i \Bigg[f_j - \frac{\epsilon_j^+}{6}\left(1 - \frac{\alpha_i}{\Delta x}\right)\left(1 + \frac{\alpha_i}{\Delta x}\right) \\ \times (f_{j+1} - f_j) - \frac{\epsilon_j^-}{6}\left(2 + \frac{\alpha_i}{\Delta x}\right)\left(1 + \frac{\alpha_i}{\Delta x}\right)(f_j - f_{j-1}) \Bigg].\end{aligned}$$

3. NUMERICAL TESTS

3.1. The Linear Advection

Let us first consider the problem of linear advection:

$$\frac{\partial f}{\partial t} + v\frac{\partial f}{\partial x} = 0, \quad \forall x \in [-\pi, \pi], \quad \text{and} \quad f(t, -\pi) = f(t, \pi). \tag{19}$$

Under these assumptions and simplifications. One can Fourier analyze the schemes using a discrete Fourier transform

$$f_j^n = \sum_{k=0}^{N-1} \hat{f}_k^n e^{ikx_j}, \quad \text{where } \hat{f}_k^n = \sum_{j=0}^{N-1} f_j^n e^{-ikx_j}.$$

Then, the solution of (19) in the Fourier space is given by

$$\hat{f}_k^n = \hat{f}_k^0 e^{ikvt^n}. \tag{20}$$

In general, Eq. (20) is not satisfied by the algorithm, so it is valuable to give the types of numerical error which can occur:

- amplitude error $\hat{f}_k^n / \hat{f}_k^0$: the harmonic must decay to stabilize the algorithm, which introduces numerical diffusion. These errors are usually most important for short-wavelength harmonics.
- phase error $|v\,t^n - Arg(\hat{f}_k^n / \hat{f}_k^0)|$: it is generally called dispersion and describes the error of harmonics which propagate at the wrong speed. The error usually increases with the wave number k.

On the one hand, the amplification factor is plotted (see Fig. 1) for the FBM and third-order reconstruction without the slope corrector (Part a), and for the semiLagrangian method

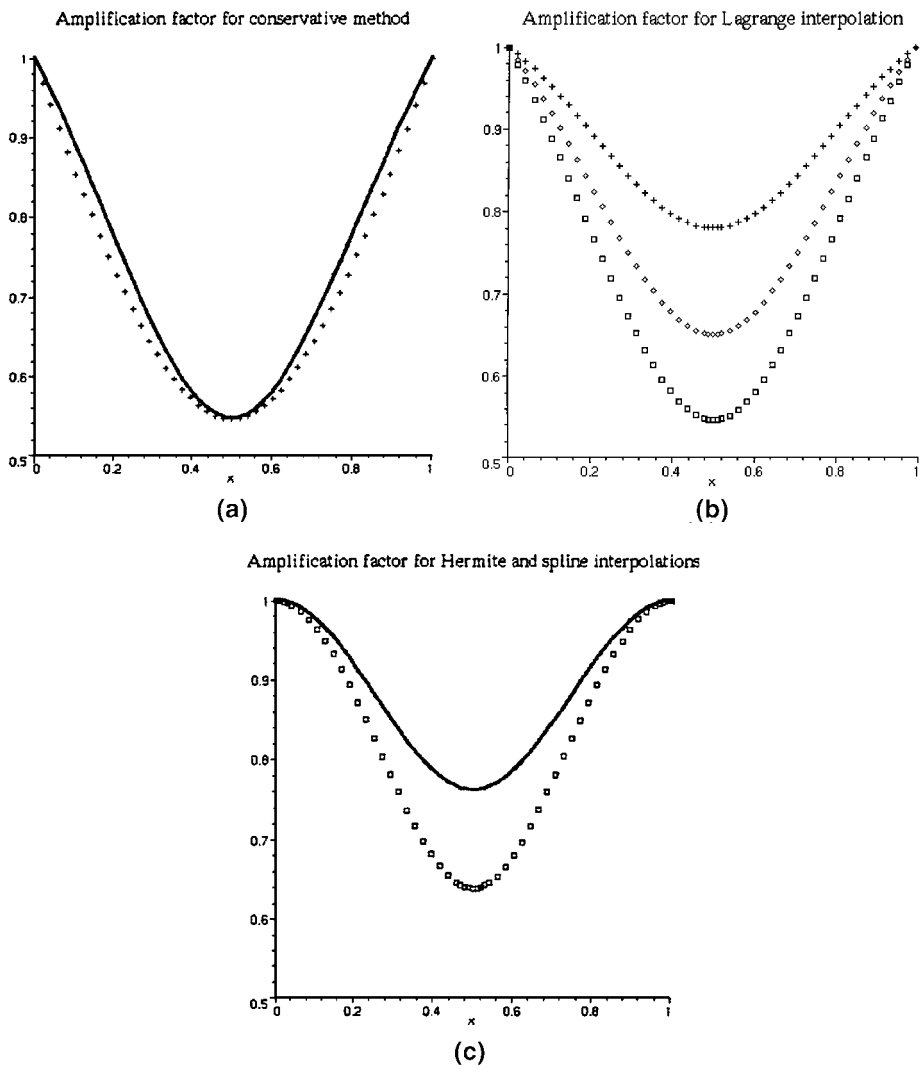

FIG. 1. The amplification factor with respect to α for a fixed mode k. (a) the classical FBM (crosses) and third-order reconstruction without slope corrector (solid line); (b) The semiLagrangian method with a Lagrange interpolation of degree 3 (boxes), 5 (diamonds), and 9 (crosses); (c) and with cubic Hermite polynomial with a fourth-order approximation of the derivative (boxes); and cubic spline interpolation (solid line).

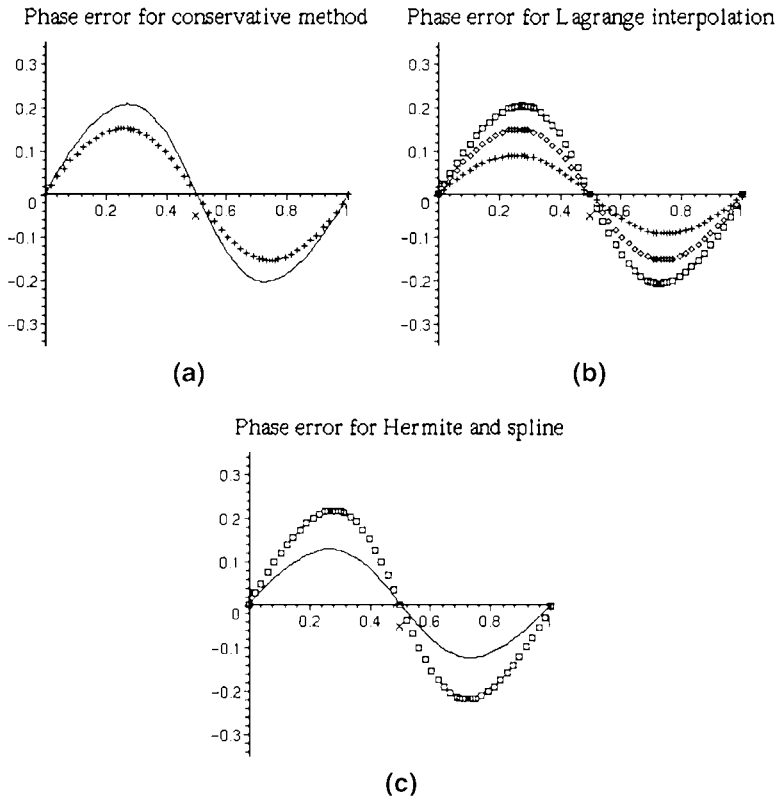

FIG. 2. The phase error with respect to α for a fixed mode k. (a) the conservative method for the classical FBM (crosses) and third-order reconstruction without slope corrector (solid line); (b) the semiLagrangian method with a Lagrange interpolation of degree 3 (boxes), 5 (diamonds), and 9 (crosses); (c) and with cubic Hermite polynomial with a fourth-order approximation of the derivative (boxes), and cubic spline interpolation (solid line).

with Lagrange (Part b), Hermite and cubic spline (Part c) interpolations. Methods using a smooth reconstruction (Hermite or cubic spline) are less dissipative than ones using only a continuous approximation. To obtain a similar amplification factor with the Lagrange interpolation, a polynom of degree nine is required. The dissipation of the conservative method with a quadratic polynom is identical to the cubic Lagrange interpolation one. The linear reconstruction used in the (FBM) is the most dissipative. On the other hand, the phase error (see Fig. 2) for the semiLagrangian method using a Hermite reconstruction with fourth-order approximation of the derivative is the most important. The cubic spline reconstruction is also less accurate than the Lagrange interpolation of degree nine.

3.2. The Vlasov–Poisson System

In this section, we want to compare different methods and reconstructions for the numerical resolution of the Vlasov–Poisson system with periodic boundary conditions,

$$\frac{\partial f}{\partial t} + \mathrm{div}_x(vf) + \mathrm{div}_v(E(t,x)\,f) = 0, \tag{21}$$

coupled with the normalized Poisson equation

$$E(t,x) = -\nabla_x \phi(t,x), \quad -\Delta\phi(t,x) = \int_{\mathbb{R}^d} f(t,x,v)\,dv - 1. \tag{22}$$

The time discretization procedure, originally proposed by Cheng and Knorr [5], is based on a splitting algorithm and can be used to go from time step t^n to t^{n+1} as follows.

1. Perform a half time step shift along the x-axis: $f^*(x,v) = f(t^n, x - v\Delta t/2, v)$.
2. Compute the electric field at time $t^{n+1/2}$ by substituting f^* in the Poisson equation.
3. Perform a shift along the v-axis: $f^{**} = f^*(x, v - E(t^{n+1/2}, x)\Delta t)$.
4. Perform a second half time step shift along the x-axis: $f(t^{n+1}, x, v) = f^{**}(x - v\Delta t/2, v)$.

We now propose classical numerical tests to compare different reconstructions.

A. *The Linear Landau Damping in 1D*

The initial data are

$$f(0,x,v) = \frac{1}{\sqrt{2\pi}} \mathrm{e}^{-v^2/2}(1 + \alpha\cos(kx)), \quad \forall (x,v) \in (0,L) \times \mathbb{R},$$

where $\alpha = 0.01$, the periodic length is $L = 4\pi$, and $k = 0.5$. We are using a number of cells $N_x = 32$ in the x-direction, and N_v = 16, 32, and 64 in the v-direction, with $v_{max} = 4.5$, and $\Delta t = 1/8$.

Figure 3 represents the evolution of the electric energy $\sum |E_i(t)|^2$ obtained by the PFC scheme, the fourth order ENO reconstruction, and the semiLagrangian method using a cubic spline interpolation with $N_v = 32$. The recurrence effect appears at $T_R = 44.68$, which is the theoretical time predicted from the free streaming case since $T_R = 2\pi/(k\Delta v)$. The PFC method first gives a good approximation of the damping rate but when approaching the recurrence time the evolution of the electric field is less accurate, whereas the behavior obtained by the fourth-order ENO scheme and the semiLagrangian method is more stable for a long time. In this case, the distribution function obtained with different schemes remains positive, and the relative error norm of variations of the kinetic entropy, L^2-norm, and total energy always stays less than 10^{-5}.

In Fig. 4, the basic mode of the electric field $k = 0.5$, obtained by the PFC method, is plotted against time for $N_v = 16$, 32, and 64 cells. It shows the exponential decay of the amplitude of the electric field according to Landau's theory. The damping rate and the frequency of oscillations obtained by this method with only 32 cells in the v direction are respectively $\gamma = 0.153$ and $\omega = 1.415$, which agree very well with values $\gamma = 0.1533$ and $\omega = 1.4156$ predicted by the theory. The use of a sufficiently large number of cells allows us to improve the time evolution of the electric field and gives good results.

B. *The Strong Landau Damping in 1D*

In this example, the amplitude of the initial perturbation of the density is increased; we take for the initial data $\alpha = 0.5$ and $v_{max} = 6$. The number of cells is $N_x = 32$ and $N_v = 64$,

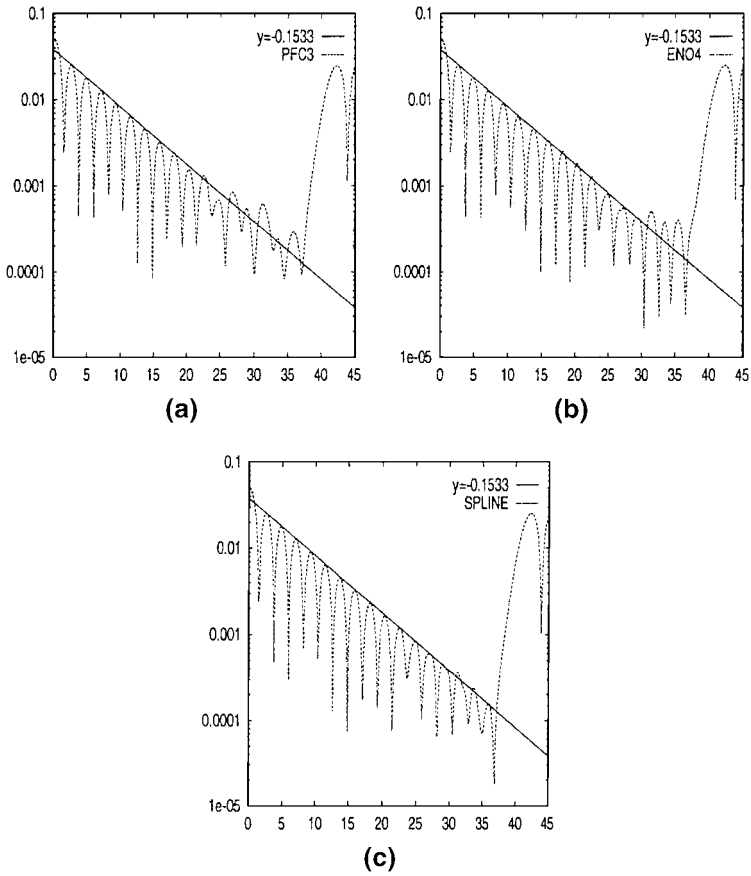

FIG. 3. Time evolution of the electric energy on logarithm scale obtained by the PFC method (a), the fourth-order ENO (b), and the cubic spline (c) interpolation with 32×32 unknowns for linear Landau damping.

128. The previous theory cannot be applied because nonlinear effects are too important, but this test has been studied by many authors [8, 10, 15]. Results are in good agreement with numerical simulations presented in the literature: the electric energy first decays exponentially and is next periodically oscillating. In Fig. 5, the evolution of the electric energy is plotted for the PFC scheme with 32×64 cells, and for the semiLagrangian method using a cubic spline interpolation with 32×64 and 32×128 points. The result obtained by the PFC method is much more accurate than the one obtained by the semiLagrangian method using the same grid.

Next, we are interested by the evolution of the kinetic entropy and L^p-norms which are theoretically conserved. The evolution of the discrete entropy $H(t) = -\sum f_i(t) \ln(f_i(t))$, and the discrete $L^p(t)$-norm $\sum |f_i(t)|^p$ for $p = 1, 2$ are presented in Fig. 6 for the various schemes. The variation of the L^1-norm represents the rate of negative values since the global mass $\sum f_i(t)$ is preserved even for semiLagrangian methods. On the one hand, the semiLagrangian method does not preserve positivity, and the amplitude of spurious oscillations increases when nonlinear effects occur. On the other hand, as is predicted by the Fourier analysis, the conservative method is more dissipative than the semiLagrangian

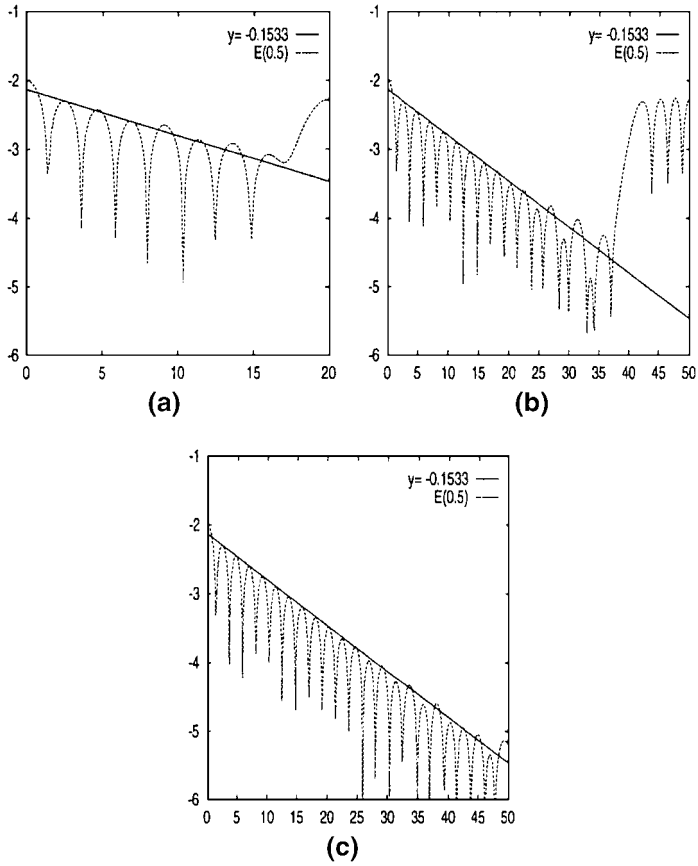

FIG. 4. Time evolution of the first mode of the electric field $E(t, k = 0.5)$ obtained by the PFC method with $N_v = 16$, $N_v = 32$, and $N_v = 64$ cells for linear Landau damping.

one since the kinetic entropy strongly decreases. The variation of the stencil of the ENO reconstruction acts as a smoothing effect, so the dissipation is much more important, and indeed the kinetic entropy is not well stabilized. The entropy obtained by the PFC scheme is at first increasing and then well stabilized, whereas with the semiLagrangian method it oscillates. The strong dissipation of the conservative method can be explained by the averaging step; indeed small details of the distribution function are eliminated to stabilize the scheme. As for the distribution function in the (x, v) space, small bumps appear around the phase velocity $v_\phi = \omega/k$. These bumps represent particles which are trapped by electrostatic waves (see Fig. 7). As a consequence of the entropy decay, the distribution function is smoothed when filaments become smaller than the phase space grid size. Nevertheless, this smooth approximation seems to give a good description of macroscopic values (physics quantities obtained by the integration of moments of the distribution function with respect to v) since the evolution of the electric energy is more accurate than the one obtained from the semiLagrangian method using the cubic spline interpolation. Moreover, the variation of the total energy is less than 2% for all schemes except for the ENO method, for which the variation of the total energy is increasing and the amplitude of the electric energy is damped. Thus, the ENO reconstruction does not seem to be well adapted to treating nonlinear effects.

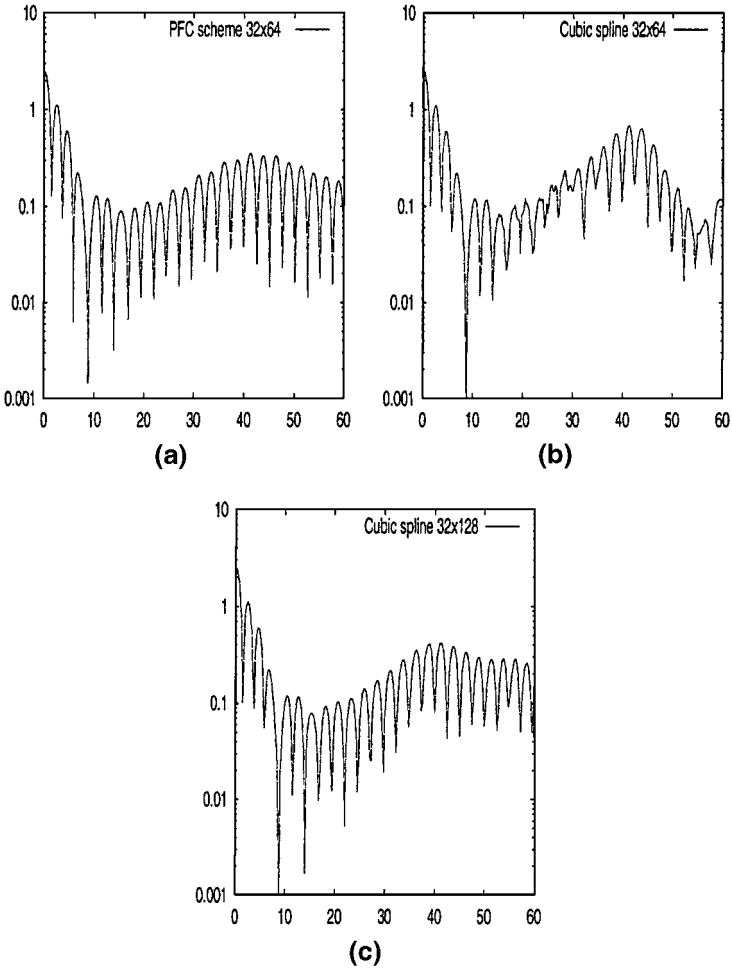

FIG. 5. Time evolution of the discrete electric energy in logarithm scale for the PFC scheme 32×64 (a); the cubic spline interpolation with 32×64 (b) 32×128 (c) unknowns for strong Landau damping.

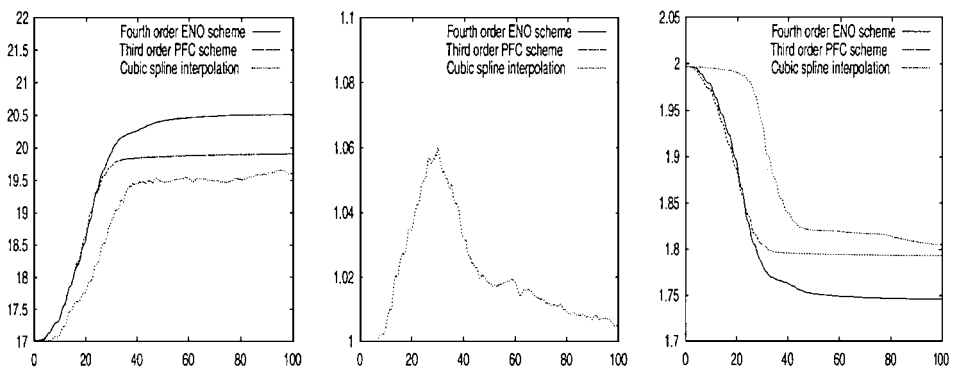

FIG. 6. Time evolution of the discrete kinetic entropy; L^1 and L^2 norms with 32×64 unknowns for strong Landau damping.

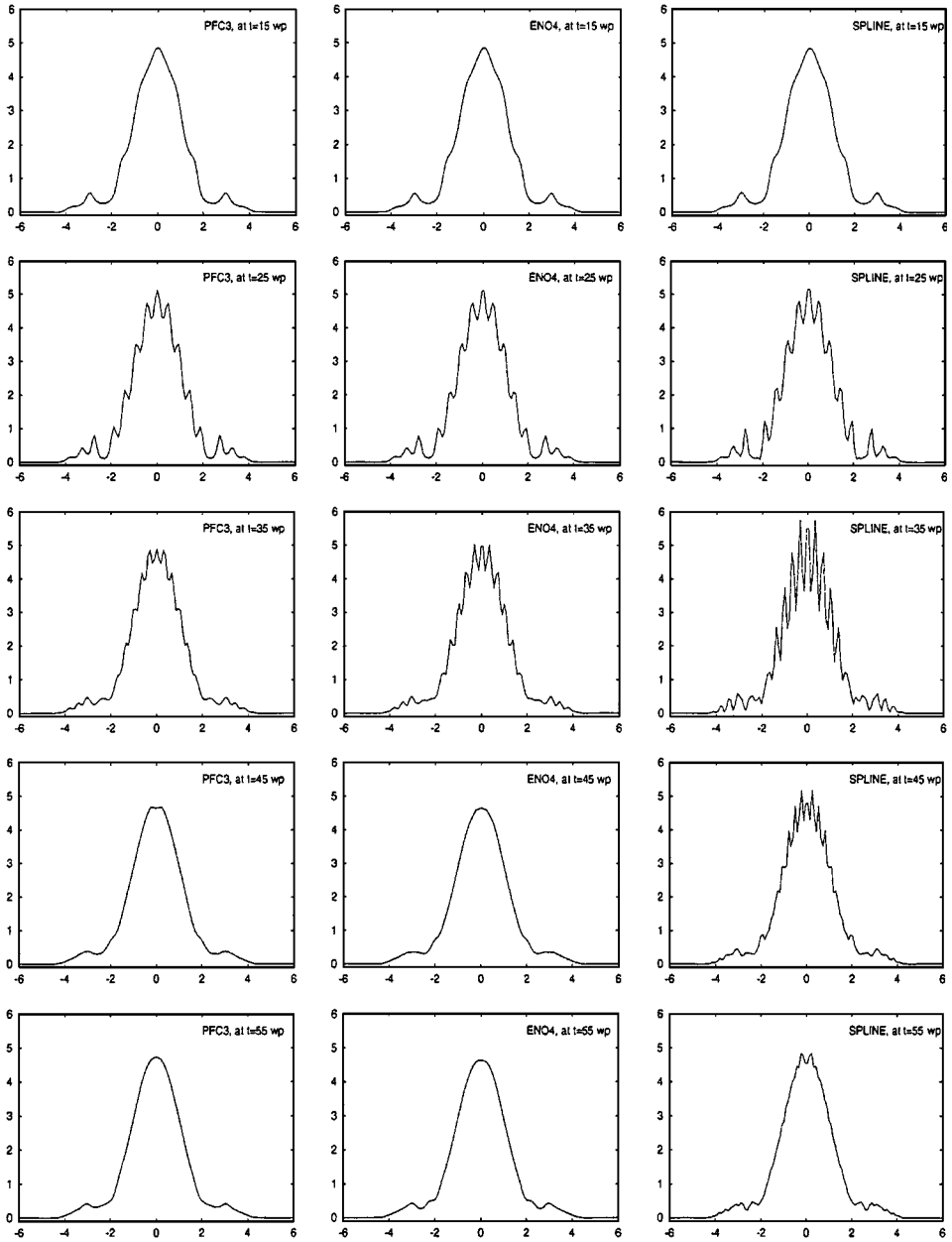

FIG. 7. Time development of the spatially integrated distribution function for the PFC scheme (left); the fourth order ENO reconstruction (center), and the cubic spline (right) interpolation for strong Landau damping.

C. *The Linear Landau Damping in 2D*

The initial condition is set to

$$f_0(x, y, v_x, v_y) = \frac{1}{2\pi} \mathrm{e}^{-(v_x^2+v_y^2)/2}(1 + \alpha \cos(k_x x) \cos(k_y y)),$$

with $\alpha = 0.05$. The velocity space is truncated at $v_{max} = 6$, the wave numbers are $k_x = k_y =$

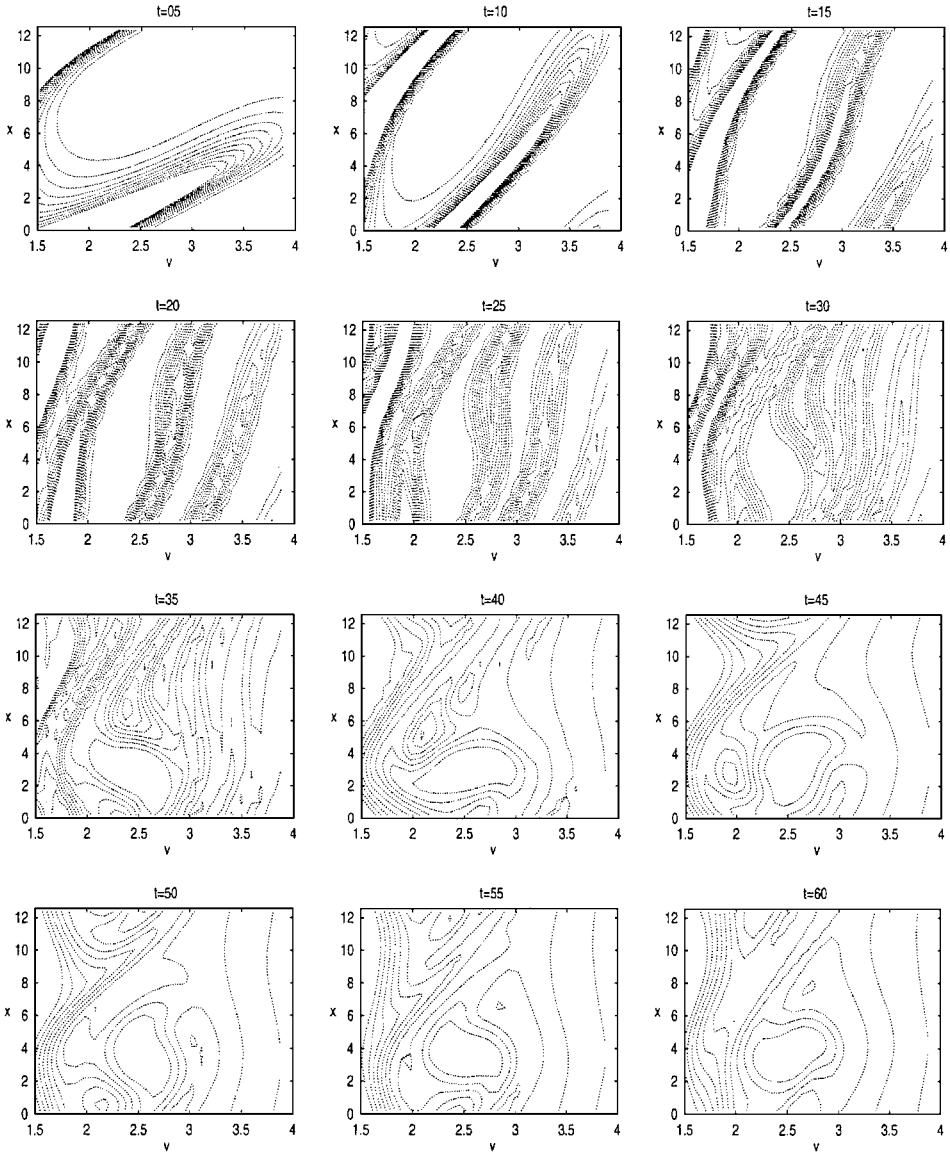

FIG. 8. Time development distribution function $f(t, x, v) \leq 0.1$ obtained by the PFC scheme for strong Landau damping.

0.5, and the length of the periodic box in the physical space is $L_x = L_y = 4\pi$. Finally, the four-dimensional grid contains 64 points per direction and the time step is set to $\Delta t = 1/8$. Because of the symmetry of the initial data, the evolution of two components of the electric field is identical. In Fig. 9, we report the evolution of the electric energy obtained by the PFC scheme and the semiLagrangian method using a cubic spline interpolation. The two methods give an accurate damping of the amplitude of the electric field. The Fourier modes of the electric field obtained by the PFC scheme are plotted in Fig. 10. It shows the exponential decay of the modes $E_x(t, k_x = 0, k_y = 0.5)$ and $E_x(t, k_x = 0.5, k_y = 0.5)$ with damping rates, respectively, $\gamma = -0.1533$ and $\gamma = -0.394$, and the frequency of

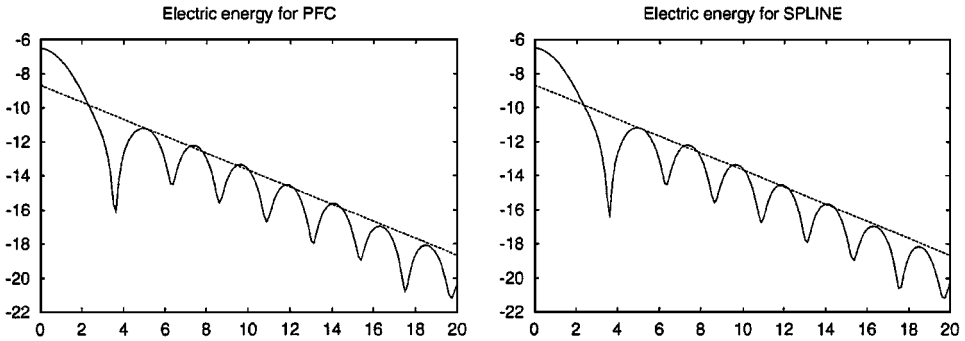

FIG. 9. Time evolution of the electric energy $(\Delta x \sum_i E_i^2)^{1/2}$ on logarithm scale obtained by the PFC and SPLINE methods with 64×64 unknowns for the 2D linear Landau damping.

oscillations $\omega = 1.4156$ and $\omega = 1.6973$, which are the theoretical values predicted by the linear Landau theory.

D. *The Evolution of a Beam in 2D*

We now consider the evolution of a root mean square (RMS) matched semiGaussian beam in a uniform focusing channel in the four-dimensional phase space. In this case the Vlasov equation has the form, for all $\mathbf{x} = (x, y)$ and $\mathbf{v} = (v_x, v_y)$,

$$\frac{\partial f}{\partial t} + \mathbf{v} \cdot \nabla_{\mathbf{x}} f + (E_{self}(t, \mathbf{x}) + E_{appl}(t, \mathbf{x})) \cdot \nabla_{\mathbf{v}} f = 0, \tag{23}$$

where E_{self} is the self-consistent electric field given by the Poisson equation and E_{appl} is a linear external electric field which allows us to focalize the beam. The initial value of the distribution function is

$$f_0(x, y, v_x, v_y) = \frac{n_0}{(2\pi v_{th}^2)(\pi a^2)} e^{-\frac{v_x^2+v_y^2}{2v_{th}^2}}, \quad \text{if } x^2 + y^2 \le a^2,$$

and $f_0(x, y, v_x, v_y) = 0$, if $x^2 + y^2 > a^2$. The RMS thermal velocity v_{th} is computed such that the beam is matched (see [11]): we consider the KV-distribution function which is a

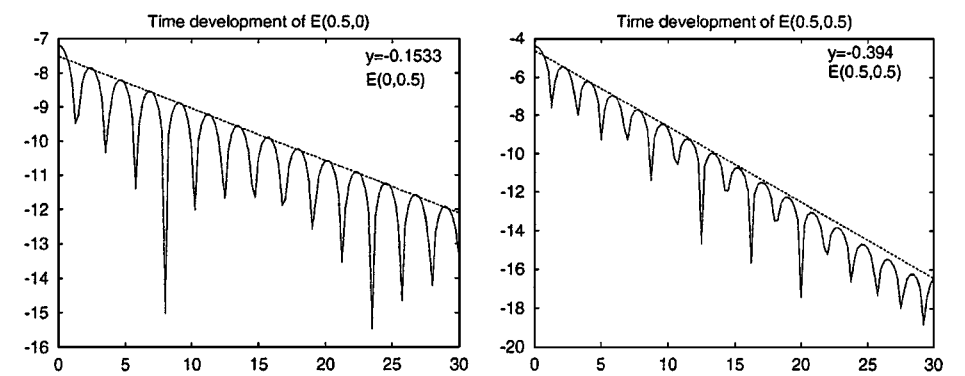

FIG. 10. Time evolution of the basic modes $E_x(0.5, 0)$ and $E_x(0.5, 0.5)$ on logarithm scale obtained by the PFC method with 64×64 unknowns for the 2D linear Landau damping.

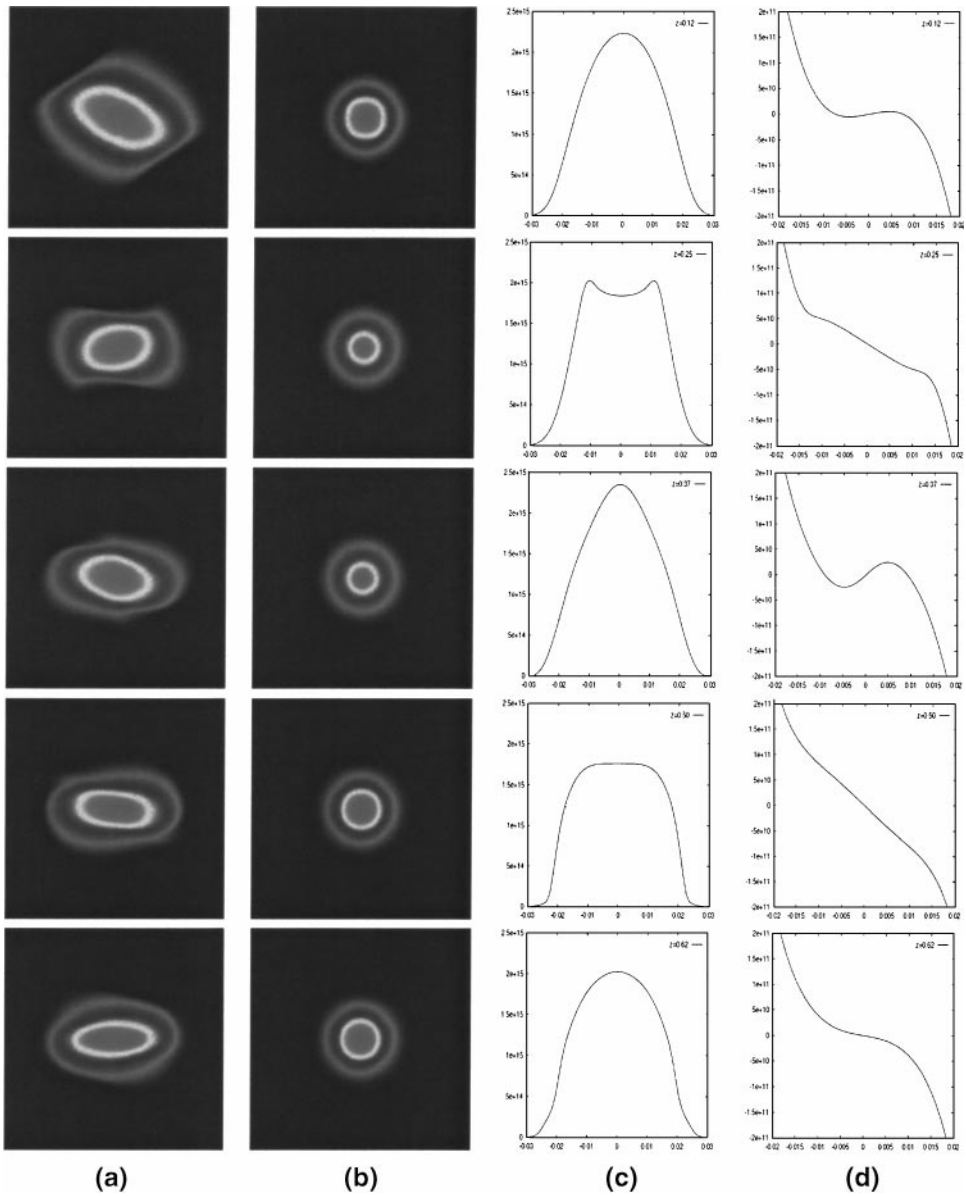

FIG. 11. Time development of (a) x–v_x projection, (b) v_x–v_y projection, (c) slice of charge density, and (d) slice of the total electric field obtained by the PFC method.

stationary solution of the Vlasov equation (23) and the self-consistent electric field is linear with respect to the x variable. Then

$$E_{self}(t, \mathbf{x}) + E_{appl}(t, \mathbf{x}) = -\omega^2 \mathbf{x}.$$

And the initial data are

$$f_0(\mathbf{x}, \mathbf{v}) = \delta_{\mathcal{C}}, \quad \text{with}\, \mathcal{C} = \left\{ \frac{x^2}{A^2} + \frac{y^2}{A^2} + \frac{v_x^2}{(\omega A)^2} + \frac{v_y^2}{(\omega A)^2} = 1 \right\}.$$

TABLE I
Total Computation Time for PFC3 and SPLINE Methods with Respect to the Number of Processors for a Grid Size $64 \times 64 \times 64 \times 64$ Points

Number of processors	PFC scheme	SPLINE method
2	4 h 30 min	6 h 20 min
4	2 h 11 min	3 h 07 min
8	56 min	84 min

Then, the RMS values are given by

$$\sqrt{\overline{x^2}} = \sqrt{\frac{\int x^2 f d\mathbf{x}\, d\mathbf{v}}{\int f d\mathbf{x}\, d\mathbf{v}}} = A, \quad \sqrt{\overline{v_x^2}} = \sqrt{\frac{\int v_x^2 f d\mathbf{x}\, d\mathbf{v}}{\int f d\mathbf{x}\, d\mathbf{v}}} = \omega A,$$

$$\sqrt{\overline{y^2}} = \sqrt{\frac{\int y^2 f d\mathbf{x}\, d\mathbf{v}}{\int f d\mathbf{x}\, d\mathbf{v}}} = A, \quad \sqrt{\overline{v_y^2}} = \sqrt{\frac{\int v_y^2 f d\mathbf{x}\, d\mathbf{v}}{\int f d\mathbf{x}\, d\mathbf{v}}} = \omega A.$$

Now, for the semiGaussian beam, the initial self-consistent electric field can be easily computed since it is also linear in **x**. Then, we take

$$\overline{x^2} = \overline{y^2} = a^2/4, \quad v_{th}^2 = \overline{v_x^2} = \overline{v_y^2} = \omega^2 a^2/4,$$

and ω^2 represents the difference between the initial self-consistent electric field and the linear applied field $E_{appl}(t, x) = -\omega_0^2 x$. In this example, we have chosen ω and ω_0 such that the tune depression $\omega/\omega_0 = 1/2$. The beam density n_0 can be written with respect to the current I and the beam velocity v_b, by $n_0 = I/q v_b$. The beam is assumed to be composed of ionized particles of potassium, the current $I = 0.2A$, the beam velocity $v_b = 0.63 \times 10^6$ m/s, and the radius of the beam is $a = 0.02$ m. We compare the evolution of the beam obtained by the PFC algorithm using the third-order positive reconstruction with the semiLagrangian method using the cubic spline interpolation (see [14]).

In Table I, we present the total time computation for the semiLagrangian method and the PFC scheme. It is evident that the PFC scheme is faster than the semiLagrangian method since the reconstruction is local. Contour plots of the phase space projections as well as slices of the charge density and the electric field obtained by the PFC method are given in the following figures. We notice that the beam at first becomes hollow, then regions of high density propagate to the core of the beam and out again, creating space charge waves. These waves are damped by phase mixing after a few lattice periods. Results obtained by the PFC method seem to be very close to those obtained by the semiLagrangian method.

4. CONCLUSION

In this paper, we introduced a new method to solve the Vlasov equation using a phase space grid. This method enforces the conservation of the global mass (or the number of particles) and controls numerical oscillations using the stencil variation technique (ENO reconstruction) or the preservation of positivity (PFC). Moreover, it allows us to treat strong nonlinear problems without numerical instabilities. On the one hand, numerical results

show that the ENO approximation is too dissipative to accurately describe the distribution function, because the entropy and the L^2 norm are strongly decreasing. On the other hand, the PFC scheme is almost as accurate as the semiLagrangian method using a cubic spline interpolation, and the preservation of positivity allows us to have a better description of macroscopic values like the charge density or the electric field over time. Moreover, the local reconstruction is well suited to doing parallel computation in high dimension.

Using today's supercomputers, this method appears to be a good alternative to the PIC methods for dealing with strongly nonlinear problems in two- or four-dimensional phase space when little noise and high precision is needed. Moreover, we have been able to perform toy simulations in the six-dimensional phase space and it is likely that the next generation of supercomputers or the use of many computers distributed over a network will soon enable us to perform physically relevant simulations on a five- or six-dimensional phase space.

REFERENCES

1. C. K. Birdsall and A. B. Langdon, *Plasma Physics via Computer Simulation* (Inst. of Phys. Publishing, Bristol/Philadelphia, 1991).
2. F. Bouchut, F. Golse, and M. Pulvirenti, *Kinetic Equations and Asymptotic Theory* (Gauthier–Villars, Paris, 2000).
3. J. P. Boris and D. L. Book, Flux-corrected transport. I: SHASTA, a fluid transport algorithm that works, *J. Comput. Phys*. **11**, 38 (1973).
4. J. P. Boris and D. L. Book, Flux-corrected transport. III: Minimal-error FCT algorithms, *J. Comput. Phys*. **20**, 397 (1976).
5. C. Z. Cheng and G. Knorr, The integration of the Vlasov equation in configuration space, *J. Comput. Phys*. **22**, 330 (1976).
6. E. Fijalkow, A numerical solution to the Vlasov equation, *Comput. Phys. Commun*. **116**, 319 (1999).
7. A. Harten and S. Osher, Uniformly high-order accurate non-oscillatory schemes. I, *SIAM J. Numer. Anal*. **24**, 279 (1987).
8. A. J. Klimas, A method for overcoming the velocity space filamentation problem in collisionless plasma model solutions, *J. Comput. Phys*. **68**, 202 (1987).
9. A. J. Klimas and W. M. Farrell, A splitting algorithm for Vlasov simulation with filamentation filtration, *J. Comput. Phys*. **110**, 150 (1994).
10. G. Manfredi, Long time behavior of nonlinear Landau damping, *Phys. Rev. Lett*. **79–15**, 2815 (1997).
11. M. Reiser, *Theory and Design of Charged Particle Beams* (Wiley, New York, 1994).
12. M. Shoucri and G. Knorr, Numerical integration of the Vlasov equation, *J. Comput. Phys*. **14–1**, 84 (1974).
13. E. Sonnendrücker, J. Roche, P. Bertrand, and A. Ghizzo, The semi-Lagrangian method for the numerical resolution of Vlasov equations, *J. Comput. Phys.* **149**, 201 (1998).
14. E. Sonnendrücker, J. J. Barnard, A. Friedman, D. P. Grote, and S. M. Lund, Simulation of heavy ion beams with a semi-Lagrangian Vlasov solver, *Proceedings of the HIF 2000 Symposium*, in Nuclear Inst. and Methods in Physics Research (Elsevier, Amsterdam, 2001) Vol. 464, p. 470.
15. T. Nakamura and T. Yabe, Cubic interpolated propagation scheme for solving the hyper-dimensional Vlasov–Poisson equation in phase space, *Comput. Phys. Commun*. **120**, 122 (1999).
16. S. I. Zaki, L. R. Gardner, and T. J. M. Boyd, A finite element code for the simulation of one-dimensional Vlasov plasmas I. Theory, *J. Comput. Phys*. **79**, 184 (1988).
17. S. I. Zaki, L. R. Gardner, and T. J. M. Boyd, A finite element code for the simulation of one-dimensional Vlasov plasmas II. Applications, *J. Comput. Phys*. **79**, 200 (1988).